

How Sparsity Allocation Shapes Label-Free Post-Pruning Recoverability

Qishi Zhan¹ Minxuan Hu² Liang He³

¹Marquette University ²Cornell University ³Tongji University

qishi.zhan@marquette.edu

Abstract

Unstructured magnitude pruning at high sparsity ratios can reduce a neural network’s accuracy to near-random performance, yet retraining with labeled data is often infeasible in practical deployment settings. Recent work on Adaptive Signal Resuscitation (ASR) shows that label-free, gradient-free channelwise repair can recover substantial accuracy from collapsed sparse models [10]. Building on this repair operator as a fixed backend, we ask a different question: how does the choice of upstream sparsity allocation affect the amount of activation signal that remains recoverable after pruning? We evaluate ERK and LAMP allocations under the same ASR repair protocol across CIFAR-10, CIFAR-100, and Imagenette with ResNet-18, ResNet-34, and ResNet-50, at sparsities from 90% to 95.5%. Our results show that allocation choice systematically changes post-repair accuracy at the same global sparsity, that a repair-sensitive transition regime exists in which BN recalibration fails but ASR still recovers nontrivial accuracy, and that the width and location of this regime vary with architecture and dataset difficulty. Additional validations on ImageNet-100 and DenseNet-121 further characterize how recoverability varies with data scale and connectivity pattern.

1 Introduction

Neural network pruning reduces inference cost by removing weights, but aggressive pruning at high sparsity can cause severe accuracy collapse, a regime in which the pruned model performs at or near random-chance levels, well beyond ordinary accuracy degradation. Recovering from this collapse typically requires fine-tuning with labeled data, which may be unavailable when models are deployed in data-restricted environments or when the original training pipeline is inaccessible.

Prior work on pruning has concentrated primarily on *how to prune*. Sparsity allocation strategies such as ERK [1] and LAMP [6] determine how density budgets are distributed across layers, and magnitude-based criteria remove weights of smallest absolute value. These methods address the allocation problem but do not specify what should be done *after* pruning, particularly in the label-free setting.

Recent work on Adaptive Signal Resuscitation (ASR) fills this gap by formulating label-free post-pruning recovery as a channelwise activation-statistic repair problem [10]. ASR estimates a variance-matching correction for each output channel and stabilizes it with a data-driven shrinkage rule, requiring only forward passes on a small calibration set. This repair operator has been shown to substantially outperform Batch-Norm (BN) recalibration at high sparsity across several architectures and datasets.

This paper asks a complementary question. Rather than asking *how* to repair a pruned model, we ask *when* a pruned model remains repairable: given a fixed label-free repair backend, how does the upstream sparsity allocation affect the amount of activation signal that survives pruning and can be recovered? We treat ASR

Post-Pruning Repair Pipeline

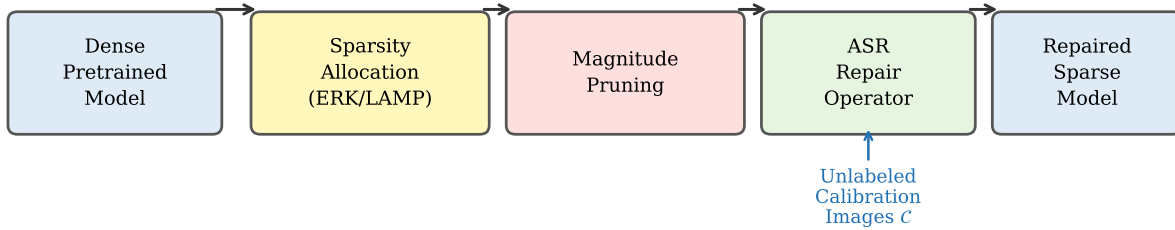


Figure 1: The post-pruning repair pipeline studied in this work. A dense pretrained model is pruned via a sparsity allocation rule (ERK or LAMP) followed by magnitude pruning. The ASR repair operator [10] is then applied as a fixed post-processing stage using only unlabeled calibration images \mathcal{C} . We study how the allocation choice affects post-repair accuracy under this fixed backend.

as a fixed repair protocol and vary only the allocation rule, examining how ERK and LAMP preserve or destroy the channelwise activation signal that ASR can exploit. This perspective shifts the focus from repair operator design to the recoverability consequences of allocation choice. Figure 1 illustrates the overall pipeline.

Contributions..

1. We study the interaction between layerwise sparsity allocation and label-free post-pruning reparability, using ASR [10] as a fixed repair backend rather than proposing a new repair operator.
2. We show that allocation choice changes the amount of recoverable activation signal left after pruning: ERK and LAMP yield substantially different post-repair accuracies at the same global sparsity, with the direction of the advantage changing across architectures and datasets.
3. We identify repair-sensitive transition regimes in which BN recalibration begins to fail but ASR still recovers nontrivial accuracy. Outside this band, either BN already performs well or the sparse model is close to irrecoverable collapse; the width and location of the transition vary with architecture, allocation, and dataset difficulty.
4. Across ResNet-18, ResNet-34, and ResNet-50 on CIFAR-10, CIFAR-100, and Imagenette, with additional ImageNet-100 and DenseNet-121 validations, we show that post-repair recoverability varies systematically with allocation, sparsity, dataset difficulty, and architecture, and that the appropriate ASR variant (aggressive versus conservative) depends on the activation landscape left by the allocation.

2 Related Work

Sparsity allocation.. ERK [1] distributes the density budget across layers using a structural rule based on layer shape. LAMP [6] derives a layer-adaptive magnitude pruning score by accounting for layerwise distortion. Both address the allocation problem but do not specify a post-pruning repair operator. This work treats ERK and LAMP as upstream allocation rules and examines how their structural differences affect the activation signal available to a fixed downstream repair stage.

Post-pruning fine-tuning.. The standard practice after pruning is to fine-tune the sparse model with labeled data and gradient-based optimization [3, 2]. This requires labeled training data and a full backward pass. Our setting prohibits both, and we treat training-based recovery as a distinct operational regime rather than a direct baseline.

BatchNorm recalibration.. Recomputing BN statistics from a calibration set without labels or gradients is a common lightweight adjustment after pruning or quantization [8]. We treat BN recalibration as the primary label-free baseline and characterize the sparsity regime in which it begins to fail, which defines the lower boundary of the repair-sensitive transition region.

Post-training quantization and calibration repair.. Nagel et al. [7] propose data-free quantization via weight equalization and bias correction. Lazarevich et al. [5] study post-training pruning through layerwise calibration, including bias correction followed by BN recalibration. These approaches target mean-shift distortion; ASR differs by addressing variance-level degradation, which we find necessary for reliable recovery in high-sparsity regimes.

Label-free post-pruning repair.. Adaptive Signal Resuscitation (ASR) proposes a channelwise repair operator for sparse vision networks, showing that matching the granularity of repair to the granularity of damage substantially improves recovery over layer-wise methods [10]. The present work uses ASR as a fixed backend and studies a different question: how does upstream allocation determine the amount of signal available for ASR to repair?

Activation-statistic correction.. Activation statistics have been used in related contexts to reduce distributional mismatch after model transformation. REPAIR renormalizes preactivations against reference statistics to mitigate variance distortion in model merging [4]. ASR shares the calibration-only philosophy but applies channelwise correction to pruning-induced activation damage. The present work does not introduce a new correction operator; instead, it uses ASR to study how allocation choices determine the activation landscape available for repair.

Concurrent weight-rescaling approaches.. Recent concurrent work proposes energy compensation for post-training LLM pruning using column-wise and row-wise weight energy ratios to rescale pruned weights [9]. That correction is weight-based and data-free, applied at moderate sparsity on transformer architectures without BatchNorm. The setting differs from ours along three axes: we use activation statistics from calibration images, target extreme sparsity regimes where activation collapse is severe, and operate on convolutional networks with BatchNorm layers.

3 Problem Setting

Let f_θ denote a dense pretrained network with parameters θ , and let $f_{\hat{\theta}}$ denote the pruned sparse model obtained by applying a sparsity allocation $\mathcal{A} \in \{\text{ERK}, \text{LAMP}\}$ followed by magnitude pruning to a target global sparsity $s \in (0, 1)$. Let $\mathcal{C} = \{x_1, \dots, x_n\}$ be a small set of unlabeled calibration images, with $n = 128$ in all experiments.

The label-free repair operator \mathcal{R}_{ASR} [10] maps $\hat{\theta}$ to repaired parameters using only \mathcal{C} and the dense reference f_θ , without labels or gradient computation. We fix \mathcal{R}_{ASR} and study how the allocation \mathcal{A} affects the post-repair accuracy $\text{acc}(f_{\mathcal{R}_{\text{ASR}}(\hat{\theta})})$ as a function of sparsity s , architecture, and dataset. This formulation isolates the allocation’s contribution to recoverability from the repair operator itself.

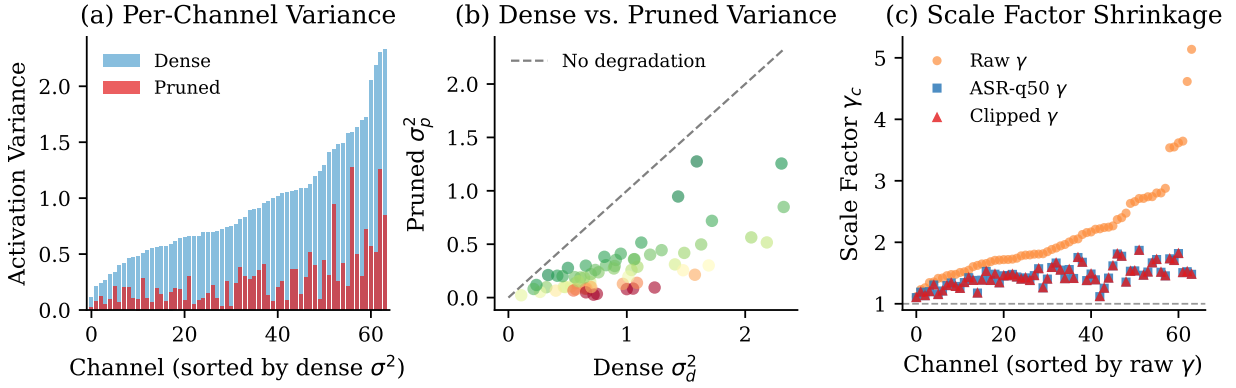


Figure 2: Per-channel variance degradation and scale factor shrinkage at 92.5% sparsity. **(a)** Per-channel activation variance before and after pruning, sorted by dense variance. **(b)** Scatter of dense versus pruned variance; channels below the diagonal have lost activation magnitude. **(c)** Comparison of raw γ_c^{raw} , shrinkage-adjusted γ_c^{q50} , and clipped γ_c^{clip} scale factors. The shrinkage prior suppresses large corrections in severely damaged channels; clipping further bounds the correction.

4 Repair Backend: Activation-Statistic Repair

We use ASR as the fixed label-free repair backend throughout this work, following Zhan et al. [10]. We summarize the repair operator below for completeness, as all allocation comparisons are evaluated after the same ASR-based repair stage.

4.1 Motivation

Pruning removes a subset of convolutional weights in each layer. For a given output channel, the surviving weights may account for only a small fraction of the original signal contribution, yielding activations with substantially lower variance than those of the dense model. When this variance reduction is severe, downstream BatchNorm layers and nonlinearities receive signals outside the range induced by the dense model, contributing to prediction collapse.

The ratio of dense-to-pruned activation variance, computed on shared calibration images, provides a channel-specific signal for how much the pruned channel’s activation scale has been degraded. Rescaling the surviving output-channel weights to partially restore this variance can meaningfully improve the sparse model’s predictions without labels or gradient updates. Figure 2 illustrates per-channel variance degradation and the effect of the two shrinkage strategies on the scale factor γ_c .

4.2 Channelwise Variance Estimation

For each convolutional layer l and output channel c , let $A_{l,c}^d$ and $A_{l,c}^p$ denote the pre-BatchNorm activations produced by the dense and pruned models on \mathcal{C} . The per-channel variances are

$$\sigma_{d,c}^2 = \text{Var} \left[A_{l,c}^d \right], \quad \sigma_{p,c}^2 = \text{Var} \left[A_{l,c}^p \right]. \quad (1)$$

The naive variance-matching scale factor for channel c is

$$\gamma_c^{\text{raw}} = \sqrt{\frac{\sigma_{d,c}^2}{\sigma_{p,c}^2 + \varepsilon}}, \quad (2)$$

where ε is a small constant for numerical stability. When $\sigma_{p,c}^2$ is very small, as occurs in nearly collapsed channels, this ratio can become large and may amplify noise rather than recover useful signal.

4.3 ASR-q50: Median-Variance Shrinkage

To attenuate noise amplification in severely damaged channels, ASR applies a shrinkage prior based on the median pruned variance across channels:

$$\lambda = \text{median}_c \{ \sigma_{p,c}^2 \}, \quad \rho_c = \frac{\sigma_{p,c}^2}{\sigma_{p,c}^2 + \lambda}. \quad (3)$$

The shrinkage-adjusted scale factor is then

$$\gamma_c^{q50} = \rho_c \cdot \gamma_c^{\text{raw}} + (1 - \rho_c). \quad (4)$$

The weight ρ_c approaches 1 for channels whose pruned variance exceeds the median and approaches 0 for the most severely damaged channels, smoothly interpolating toward no correction at the extremes.

4.4 Clipped ASR: Conservative Correction

In severe collapse regimes, ASR-q50 may still over-correct certain channels. Clipped ASR constrains the scale factor by

$$\gamma_c^{\text{clip}} = \text{clamp}(\gamma_c^{q50}, 0.5, 2.0). \quad (5)$$

The bounds $[0.5, 2.0]$ prevent any channel from being scaled by more than a factor of two in either direction, trading peak recovery magnitude for stability. The two variants represent complementary points in the aggressiveness-stability tradeoff; comparing their relative performance under different allocations is one way to characterize the activation landscape left by the allocation.

4.5 Weight Rescaling and BN Recalibration

After computing γ_c , the surviving weights of output channel c are rescaled and the bias term is adjusted to align the repaired activation mean with the dense activation mean:

$$\hat{w}_{l,c} \leftarrow \gamma_c w_{l,c}, \quad (6)$$

$$\hat{b}_{l,c} \leftarrow \gamma_c b_{l,c} + \mu_{l,c}^d - \gamma_c \mu_{l,c}^p, \quad (7)$$

where $\mu_{l,c}^d$ and $\mu_{l,c}^p$ are the dense and pruned activation means for channel c on \mathcal{C} . If the original convolution has no bias term, we set $b_{l,c} = 0$ and insert the repaired bias. A BN recalibration pass over 20 mini-batches of unlabeled images then updates each BatchNorm layer’s running statistics. The complete procedure requires only forward passes and involves no gradient computation.

5 Experimental Setup

Architectures and datasets. Main experiments are conducted on ResNet-18, ResNet-34, and ResNet-50 across CIFAR-10, CIFAR-100, and Imagenette. Two additional validations extend the scope: an ImageNet-100 experiment with ResNet-18, and a DenseNet-121 experiment on CIFAR-10 and CIFAR-100 as a non-residual architecture check.

Sparsity allocations.. Two standard allocations are compared: ERK [1] and LAMP [6]. Unstructured magnitude pruning is applied at the target global sparsity. Both allocations are evaluated under the same ASR repair protocol so that any differences in post-repair accuracy are attributable to the allocation rather than the repair operator.

Target sparsities.. For ResNet-50, CIFAR-10 and Imagenette are evaluated at 90.0%, 92.5%, and 95.0% sparsity, while CIFAR-100 is evaluated at 92.5%, 95.0%, and 95.5%. For ResNet-18 and ResNet-34, all three datasets are evaluated at 90.0%, 92.5%, and 95.0%. The ImageNet-100 validation uses the same three levels. The DenseNet-121 evaluation on CIFAR-10 uses 90.0%, 92.5%, and 95.0%; the CIFAR-100 evaluation uses 70.0%, 80.0%, 85.0%, and 90.0% to capture the transition into collapse, which occurs at lower sparsity for this architecture.

Calibration.. All repair methods use $n = 128$ unlabeled images drawn from the training set. BN recalibration uses 20 mini-batches. No labels and no gradient updates are used at any point during repair.

Baselines.. Four label-free repair strategies are compared alongside the two ASR variants: (i) *No repair*, direct evaluation of the pruned model; (ii) *BN only*, BN recalibration with no weight modification; (iii) *Bias correction + BN*, per-channel mean-shift correction followed by BN recalibration; and (iv) *Affine calibration + BN*, per-channel affine output calibration followed by BN recalibration.

6 Results

Aggregating over the 54 main ResNet allocation-sparsity settings, the best ASR variant improves over BN-only repair in every condition. The mean gain over BN recalibration is 17.4 percentage points, with a minimum gain of 1.3 points. ASR also outperforms the strongest simple calibration baseline in all 54 settings, with an average margin of 13.6 points. These aggregate results establish that ASR provides a stable repair backend across the main allocation grid, making it meaningful to analyze how upstream allocation changes post-repair recoverability.

6.1 Repair Comparison Under Fixed Allocation

Table 1 compares label-free repair methods under both ERK and LAMP allocations across all three ResNet architectures, isolating the repair operator by holding the upstream pruning allocation fixed. Figure 3 summarizes the ResNet-50 results visually.

CIFAR-10.. On ResNet-50 at 92.5% sparsity, BN recalibration reaches 20.72%, while ASR-q50 and Clipped ASR reach 67.96% and 61.59%, gains of approximately 47 and 41 percentage points over BN only. Bias correction (11.79%) and affine calibration (10.00%, near random chance) both fail substantially. ResNet-34 presents a notably different pattern: affine calibration reaches 87.24% at 92.5%, outperforming the BN-only baseline of 62.07%, yet ASR-q50 still leads at 89.27%. On ResNet-18, BN only reaches 33.95% at 92.5%, while ASR-q50 reaches 66.79% and Clipped ASR reaches 63.33%. ASR-q50 is generally stronger than Clipped ASR on CIFAR-10, consistent with the interpretation that the allocation leaves enough recoverable signal for aggressive correction to be stable.

CIFAR-100.. On ResNet-50 at 92.5% sparsity, the pruned model achieves 1.00% without repair. BN recalibration raises this to only 4.70%, marking the entry into the repair-sensitive regime; ASR-q50 reaches 21.85% and Clipped ASR reaches 25.96%. Affine calibration nearly universally fails. ResNet-34 shows

ResNet-50 with LAMP Allocation: Label-Free Repair Comparison

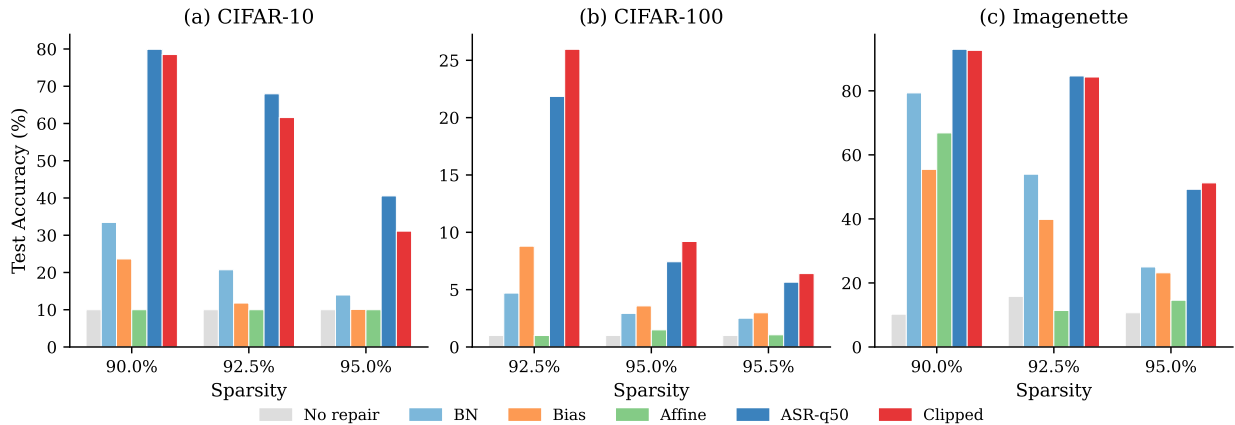


Figure 3: Repair comparison on ResNet-50 with LAMP allocation across CIFAR-10, CIFAR-100, and Imagenette. ASR-q50 and Clipped ASR consistently outperform all four baselines across sparsity levels. The large gap over BN-only recalibration marks the repair-sensitive regime.

notably stronger recovery across all methods; at 90.0% under LAMP, BN only reaches 44.96% and ASR-q50 reaches 59.81%. On ResNet-18 under LAMP at 92.5%, BN only reaches 18.45%, ASR-q50 reaches 26.48%, and Clipped ASR reaches 26.31%. On ResNet-18 and ResNet-50, Clipped ASR is competitive with or stronger than ASR-q50 on CIFAR-100, suggesting that the allocation leaves a more fragile activation landscape on these architectures at high sparsity.

Imagenette.. Both ASR variants produce strong recovery across architectures. On ResNet-50 at 92.5% under LAMP, BN only reaches 53.96%, while ASR-q50 and Clipped ASR reach 84.64% and 84.31%. On ResNet-18, BN only already reaches 83.82%, and ASR-q50 and Clipped ASR improve further to 88.84% and 89.20%, confirming that ASR provides gains even when the BN baseline is relatively strong. ResNet-34 at 92.5% under LAMP shows ASR-q50 and Clipped ASR reaching 90.04% and 90.34%, compared to 84.23% for BN only.

6.2 Allocation-Repair Interaction

Table 2 directly compares ERK and LAMP under the same ASR repair backend, making allocation the only variable. This is the central comparison for studying how allocation affects recoverability. Figure 4 presents the ResNet-18 results as line plots across sparsity levels.

CIFAR-10.. On ResNet-50, LAMP consistently yields higher post-repair accuracy than ERK at the same sparsity: at 90.0%, LAMP + ASR-q50 reaches 79.92% versus 70.24% for ERK + ASR-q50, a gap of nearly 10 points. ResNet-34 tells a different story: LAMP + ASR-q50 and ERK + ASR-q50 are nearly tied at 90.0% (90.43% versus 90.12%), but ERK begins to pull ahead at 95.0% (85.47% versus 85.81%), suggesting that ERK’s more uniform layer-level density preserves more repairable signal at the highest sparsities on this architecture. On ResNet-18, LAMP is also slightly stronger at all three levels.

CIFAR-100.. The allocation dependence is sharpest on CIFAR-100, the most challenging dataset. On ResNet-50 at 92.5%, LAMP + Clipped ASR reaches 25.96% versus 20.69% for ERK + Clipped ASR, a 5.3-point gap from allocation alone. The direction reverses on ResNet-34: ERK + ASR-q50 leads at every

Table 1: Repair comparison under fixed ERK and LAMP allocations across ResNet depths. Best result in each row is **bold**.

Arch	Dataset	Sparsity	Alloc.	No repair	BN	Bias	Affine	ASR-q50	Clip
ResNet-18	CIFAR-10	90.0%	ERK	10.00	59.39	42.76	17.99	76.92	75.39
		90.0%	LAMP	10.44	63.87	62.16	53.16	79.91	78.55
		92.5%	ERK	10.00	32.78	18.54	10.00	61.97	59.02
		92.5%	LAMP	10.00	33.95	46.13	17.89	66.79	63.33
		95.0%	ERK	10.00	14.73	13.04	10.00	34.04	31.99
		95.0%	LAMP	10.00	13.59	16.45	10.00	41.05	36.20
	CIFAR-100	90.0%	ERK	1.14	31.82	9.08	1.90	38.13	38.11
		90.0%	LAMP	1.44	33.68	12.64	5.92	40.09	40.25
		92.5%	ERK	1.11	17.26	2.69	1.12	24.34	24.19
		92.5%	LAMP	1.17	18.45	6.71	1.18	26.48	26.31
		95.0%	ERK	0.95	7.06	1.44	1.00	9.40	9.45
		95.0%	LAMP	1.06	5.72	2.55	1.00	10.96	10.89
	Imagenette	90.0%	ERK	18.90	90.04	74.45	44.23	91.87	92.00
		90.0%	LAMP	20.82	91.69	79.52	82.37	92.94	93.15
		92.5%	ERK	13.68	82.09	36.82	11.90	86.01	86.24
		92.5%	LAMP	17.50	83.82	46.47	17.48	88.84	89.20
		95.0%	ERK	10.47	58.27	16.61	9.10	68.51	68.66
		95.0%	LAMP	10.19	60.69	11.92	9.10	73.10	73.20
ResNet-34	CIFAR-10	90.0%	ERK	22.21	84.50	70.22	88.79	90.12	89.87
		90.0%	LAMP	15.34	80.34	70.29	89.53	90.43	89.89
		92.5%	ERK	17.09	72.02	47.57	85.63	89.05	88.15
		92.5%	LAMP	11.65	62.07	50.96	87.24	89.27	87.12
		95.0%	ERK	12.46	39.16	29.10	72.26	85.47	81.57
		95.0%	LAMP	10.34	28.93	35.38	75.57	85.81	77.09
	CIFAR-100	90.0%	ERK	3.73	49.77	23.87	55.68	61.38	61.02
		90.0%	LAMP	3.59	44.96	20.16	55.62	59.81	58.88
		92.5%	ERK	2.02	33.32	10.87	46.18	55.25	54.30
		92.5%	LAMP	2.28	27.58	8.66	42.68	51.83	49.64
		95.0%	ERK	1.85	13.17	4.02	26.30	41.20	40.34
		95.0%	LAMP	1.95	10.93	4.53	24.66	38.07	35.50
	Imagenette	90.0%	ERK	31.67	89.73	50.83	87.52	91.06	91.03
		90.0%	LAMP	39.26	89.20	39.39	89.53	90.83	90.96
		92.5%	ERK	13.86	86.45	19.77	80.20	90.09	90.19
		92.5%	LAMP	27.01	84.23	14.06	85.81	90.04	90.34
		95.0%	ERK	10.55	73.43	10.34	55.87	88.00	88.28
		95.0%	LAMP	16.25	66.78	10.11	66.93	87.80	88.15
ResNet-50	CIFAR-10	90.0%	ERK	10.00	28.19	10.58	10.00	70.24	64.81
		90.0%	LAMP	10.00	33.44	23.63	10.00	79.92	78.51
		92.5%	ERK	10.00	19.02	12.82	10.00	54.56	47.85
		92.5%	LAMP	10.00	20.72	11.79	10.00	67.96	61.59
		95.0%	ERK	10.00	15.08	9.38	10.00	33.87	31.62
		95.0%	LAMP	10.00	13.95	10.09	10.00	40.55	31.10
	CIFAR-100	92.5%	ERK	1.63	5.70	4.63	1.00	18.88	20.69
		92.5%	LAMP	1.00	4.70	8.79	1.00	21.85	25.96
		95.0%	ERK	1.00	2.48	1.55	1.00	7.13	8.68
		95.0%	LAMP	1.00	2.93	3.58	1.49	7.43	9.20
		95.5%	ERK	1.00	2.12	1.60	1.23	5.45	7.04
		95.5%	LAMP	1.00	2.51	2.98	1.06	5.65	6.40
	Imagenette	90.0%	ERK	13.71	65.35	26.96	17.43	88.38	89.10
		90.0%	LAMP	10.24	79.34	55.47	66.85	92.97	92.64
		92.5%	ERK	10.68	44.51	16.79	19.80	75.52	75.87
		92.5%	LAMP	15.80	53.96	39.85	11.39	84.64	84.31
		95.0%	ERK	10.68	16.64	15.80	9.91	44.33	44.05
		95.0%	LAMP	10.68	24.99	23.16	14.60	49.25	51.24

Table 2: Allocation-repair interaction: ERK versus LAMP under a fixed ASR repair backend across ResNet depths. Best result in each row is **bold**.

Arch	Dataset	Sparsity	ERK+BN	ERK+q50	ERK+Clip	LAMP+BN	LAMP+q50	LAMP+Clip
ResNet-18	CIFAR-10	90.0%	59.39	76.92	75.39	63.87	79.91	78.55
		92.5%	32.78	61.97	59.02	33.95	66.79	63.33
		95.0%	14.73	34.04	31.99	13.59	41.05	36.20
	CIFAR-100	90.0%	31.82	38.13	38.11	33.68	40.09	40.25
		92.5%	17.26	24.34	24.19	18.45	26.48	26.31
		95.0%	7.06	9.40	9.45	5.72	10.96	10.89
	Imagenette	90.0%	90.04	91.87	92.00	91.69	92.94	93.15
		92.5%	82.09	86.01	86.24	83.82	88.84	89.20
		95.0%	58.27	68.51	68.66	60.69	73.10	73.20
ResNet-34	CIFAR-10	90.0%	84.50	90.12	89.87	80.34	90.43	89.89
		92.5%	72.02	89.05	88.15	62.07	89.27	87.12
		95.0%	39.16	85.47	81.57	28.93	85.81	77.09
	CIFAR-100	90.0%	49.77	61.38	61.02	44.96	59.81	58.88
		92.5%	33.32	55.25	54.30	27.58	51.83	49.64
		95.0%	13.17	41.20	40.34	10.93	38.07	35.50
	Imagenette	90.0%	89.73	91.06	91.03	89.20	90.83	90.96
		92.5%	86.45	90.09	90.19	84.23	90.04	90.34
		95.0%	73.43	88.00	88.28	66.78	87.80	88.15
ResNet-50	CIFAR-10	90.0%	28.19	70.24	64.81	33.44	79.92	78.51
		92.5%	19.02	54.56	47.85	20.72	67.96	61.59
		95.0%	15.08	33.87	31.62	13.95	40.55	31.10
	CIFAR-100	92.5%	5.70	18.88	20.69	4.70	21.85	25.96
		95.0%	2.48	7.13	8.68	2.93	7.43	9.20
		95.5%	2.12	5.45	7.04	2.51	5.65	6.40
	Imagenette	90.0%	65.35	88.38	89.10	79.34	92.97	92.64
		92.5%	44.51	75.52	75.87	53.96	84.64	84.31
		95.0%	16.64	44.33	44.05	24.99	49.25	51.24

sparsity level (61.38% versus 59.81% at 90.0%, widening to 41.20% versus 38.07% at 95.0%). This reversal indicates that which allocation preserves more recoverable signal depends on architecture, and cannot be determined from global sparsity alone.

Imagenette. LAMP allocations generally preserve more repairable signal than ERK on both ResNet-18 and ResNet-50. On ResNet-18 at 95.0%, LAMP + ASR-q50 reaches 73.10% versus 68.51% for ERK + ASR-q50. The gap is smaller on Imagenette than on CIFAR-100, consistent with the interpretation that easier tasks leave more residual signal regardless of allocation, reducing allocation sensitivity.

6.3 ImageNet-100 Validation

Table 3 reports results on ImageNet-100 with ResNet-18. Both ASR variants consistently lead across all six conditions. The margins over BN only are smaller than on CIFAR-100 at comparable sparsity, consistent with the interpretation that ImageNet-scale models retain more distributed signal per channel, leaving less room for variance-based correction to act and narrowing the repair-sensitive transition region. The ERK-LAMP gap is also smaller than on CIFAR-100, suggesting that allocation sensitivity contracts when more residual signal survives pruning.

ResNet-18: Allocation-Repair Pipeline Comparison

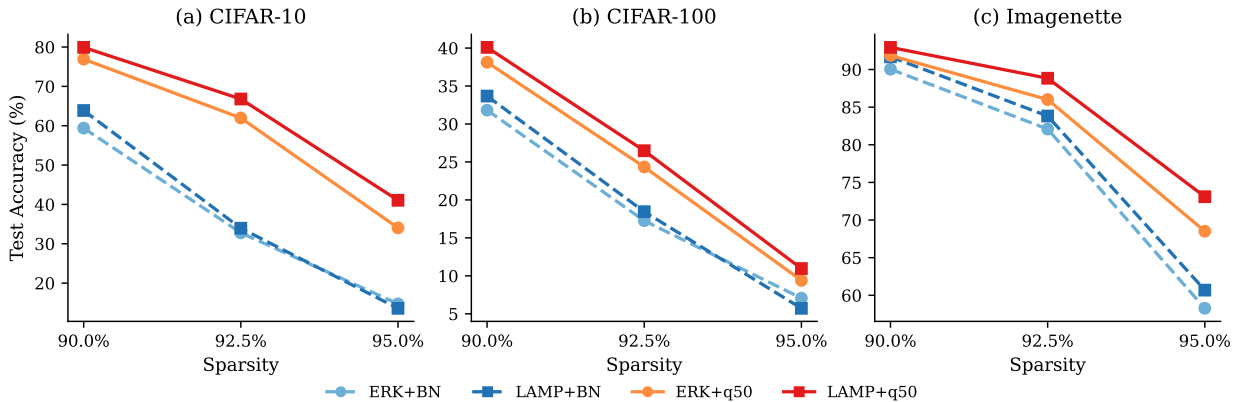


Figure 4: Allocation-repair interaction on ResNet-18 across CIFAR-10, CIFAR-100, and Imagenette. Solid lines correspond to ASR-q50-repaired models; dashed lines correspond to BN-only baselines. The gap between ERK and LAMP post-repair accuracy varies across datasets and sparsity levels, demonstrating that allocation choice shapes recoverability.

Table 3: ImageNet-100 validation on ResNet-18. Best result in each row is **bold**.

Sparsity	Alloc.	No repair	BN	Bias	Affine	ASR-q50	Clip
90.0%	ERK	2.02	48.96	41.61	7.91	49.01	49.48
90.0%	LAMP	2.78	49.75	43.83	24.81	49.75	50.17
92.5%	ERK	1.63	31.59	15.90	0.99	32.75	33.00
92.5%	LAMP	1.97	30.99	21.94	2.17	32.13	32.71
95.0%	ERK	1.00	13.15	1.87	0.93	13.88	14.01
95.0%	LAMP	1.15	11.95	5.21	1.26	13.10	13.20

6.4 DenseNet-121 Validation

Tables 4 and 5 report results on DenseNet-121, probing whether the allocation-repair interaction observed on ResNet architectures extends to non-residual connectivity. On CIFAR-10, Clipped ASR provides substantial recovery at all three sparsity levels and leads ASR-q50 throughout, reversing the ResNet-18 pattern and indicating that DenseNet-121’s dense connectivity leaves an activation landscape where aggressive correction overshoots. This architecture-dependent variant preference is itself a consequence of how allocation interacts with connectivity structure.

On CIFAR-100, the repair-sensitive transition regime occurs at substantially lower sparsity than in the ResNet experiments. At 70.0% under LAMP, BN only reaches 37.76% and Clipped ASR reaches 49.76%; the regime contracts sharply by 80.0%, where BN only manages 3.81% under LAMP while Clipped ASR still recovers 31.82%. At 85.0% and 90.0%, the transition has passed and all methods except Clipped ASR fall to near-random. This earlier onset of irrecoverable collapse demonstrates that the allocation-repair transition boundary is architecture-dependent and cannot be predicted from ResNet results alone.

7 Discussion

Allocation choice shapes the activation landscape available for repair. The ERK versus LAMP comparison under a fixed ASR backend demonstrates that allocation is not allocation-agnostic from the repair perspective. LAMP generally preserves more repairable signal on ResNet-18 and ResNet-50, but ERK is

Table 4: DenseNet-121 validation on CIFAR-10. Best result in each row is **bold**.

Sparsity	Alloc.	No repair	BN	Bias	Affine	ASR-q50	Clip
90.0%	ERK	10.00	10.99	10.00	10.26	17.43	49.48
90.0%	LAMP	10.00	10.21	10.00	11.89	15.02	28.82
92.5%	ERK	10.00	11.00	10.00	11.51	15.23	40.36
92.5%	LAMP	10.00	10.00	10.00	10.45	17.75	31.87
95.0%	ERK	10.00	11.78	10.00	10.25	10.03	38.07
95.0%	LAMP	10.00	10.00	10.00	14.08	10.00	32.02

Table 5: DenseNet-121 validation on CIFAR-100. Best result in each row is **bold**.

Sparsity	Alloc.	No repair	BN	Bias	Affine	ASR-q50	Clip
70.0%	ERK	3.27	26.98	7.46	10.11	34.64	36.57
70.0%	LAMP	11.17	37.76	11.93	31.74	49.63	49.76
80.0%	ERK	1.02	2.68	2.49	3.38	6.73	13.10
80.0%	LAMP	1.01	3.81	1.03	10.88	24.66	31.82
85.0%	ERK	1.00	1.13	1.58	2.62	1.16	5.86
85.0%	LAMP	1.00	1.04	1.00	3.60	4.45	14.72
90.0%	ERK	1.00	1.00	1.00	1.00	1.00	2.85
90.0%	LAMP	1.00	1.00	1.00	2.31	1.84	4.20

consistently stronger on ResNet-34 / CIFAR-100. This architecture- and dataset-dependent reversal suggests that the structural properties of an allocation (how it distributes density across layer sizes and types) interact with the architecture’s connectivity in ways that determine how much channelwise variance survives at any given global sparsity.

The repair-sensitive transition regime.. Across all conditions, a consistent pattern emerges: a sparsity range in which BN recalibration begins to fail but ASR still recovers nontrivial accuracy. On ResNet-50 / CIFAR-100, this transition occurs around 92–93% sparsity; on DenseNet-121 / CIFAR-100, it occurs around 70–80%. Within the transition, the choice of allocation matters most, because marginal differences in preserved channelwise variance translate into large differences in post-repair accuracy. Outside the transition (either below it, where BN already works well, or above it, where all methods collapse), allocation sensitivity contracts.

The appropriate ASR variant depends on the allocation.. ASR-q50 leads on CIFAR-10 across ResNet architectures, where the allocation leaves enough recoverable signal for aggressive correction to be stable. Clipped ASR leads on CIFAR-100 at high sparsity and on DenseNet-121 throughout, where the activation landscape after allocation is more fragile. The relative ordering of the two variants therefore provides indirect evidence about the character of the activation landscape that the allocation produces.

ASR is not a substitute for labeled fine-tuning.. ASR occupies a distinct operational regime. Masked fine-tuning, which retrains the sparse model with labeled data and gradient updates while preserving the pruning mask, substantially outperforms ASR when it is available. At 92.5% sparsity on CIFAR-100 under LAMP, Clipped ASR reaches 25.96%, while one epoch of masked fine-tuning reaches 71.49%. ASR is appropriate when labels are unavailable and computational cost must be kept low.

Sensitivity to clip bounds.. Figure 5 reports test accuracy on ResNet-18 / CIFAR-100 under four clip bound configurations: [0.25, 4.00], [0.50, 2.00], [0.67, 1.50], and [0.80, 1.25]. The two wider settings perform similarly and both improve over ASR-q50 in several conditions, while tighter bounds progressively

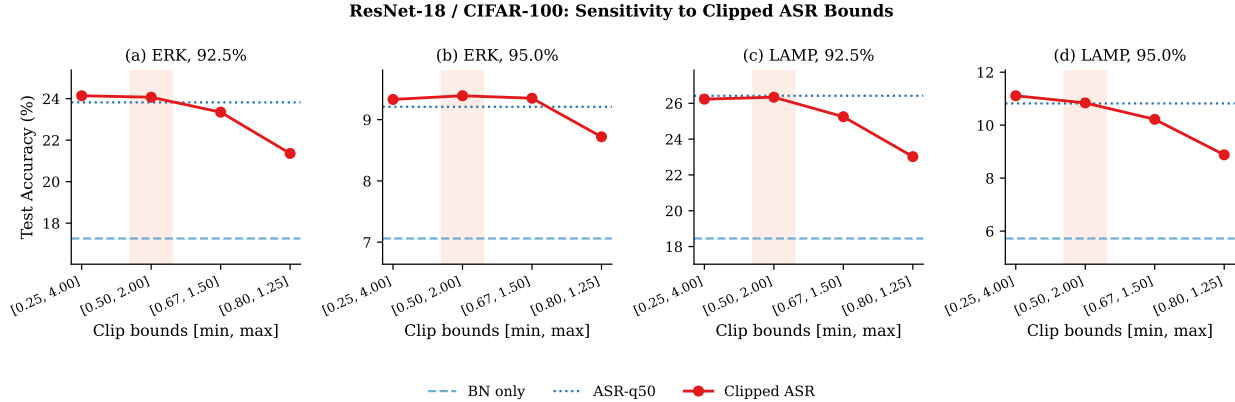


Figure 5: Sensitivity of Clipped ASR to clip bounds on ResNet-18 / CIFAR-100 under ERK and LAMP at 92.5% and 95.0% sparsity. The shaded column marks the default [0.50, 2.00] setting. Performance is stable across the two widest configurations and degrades only when bounds are tightened substantially.

reduce accuracy, most visibly under LAMP at 92.5% sparsity where [0.80, 1.25] drops 3.4 percentage points below ASR-q50. The default [0.50, 2.00] bound sits in a flat region of this sensitivity curve, suggesting that the exact value is not critical provided it is not set too conservatively.

8 Limitations and Future Work

The variance-ratio mechanism assumes that the dense model’s activation statistics serve as an appropriate repair target, an assumption that may not hold when the calibration distribution differs substantially from the test distribution. The DenseNet-121 results indicate that the repair-sensitive transition boundary varies substantially across architectures; a principled characterization of this threshold, potentially in terms of per-layer sparsity distribution or surviving activation variance, would be a useful direction for future work. The present analysis is also limited to ERK and LAMP; other allocation strategies (e.g., magnitude-based global pruning without a structural rule, or learned allocation) may exhibit different recoverability profiles. Comparisons against full post-training pruning pipelines in aligned experimental settings remain to be conducted.

9 Conclusion

We have studied how upstream sparsity allocation affects the recoverability of pruned neural networks under a fixed label-free repair backend. Using ASR as the repair operator [10], we show that ERK and LAMP allocations yield substantially different post-repair accuracies at the same global sparsity, that the direction of the advantage reverses across architectures and datasets, and that a repair-sensitive transition regime exists in which allocation choice matters most. Additional validations on ImageNet-100 and DenseNet-121 confirm that the transition boundary and the appropriate repair aggressiveness are architecture-dependent. These results suggest that allocation and repair are not independent design choices: the structural properties of the allocation determine the channelwise activation landscape available for repair, and understanding this interaction is necessary for reliably deploying label-free post-pruning recovery in practice.

References

[1] Utku Evci, Trevor Gale, Jacob Menick, Pablo Samuel Castro, and Erich Elsen. Rigging the lottery: Making all tickets winners. In *Proceedings of the 37th International Conference on Machine Learning*,

- pages 2943–2952. PMLR, 2020.
- [2] Jonathan Frankle and Michael Carlin. The lottery ticket hypothesis: Finding sparse, trainable neural networks. *International Conference on Learning Representations*, 2019.
 - [3] Song Han, Jeff Pool, John Tran, and William J. Dally. Learning both weights and connections for efficient neural networks. In *Advances in Neural Information Processing Systems*, volume 28, 2015.
 - [4] Keller Jordan, Hanie Sedghi, Olga Saukh, Rahim Entezari, and Behnam Neyshabur. REPAIR: RENormalizing permuted activations for interpolation repair. In *International Conference on Learning Representations*, 2023.
 - [5] Ivan Lazarevich, Alexander Kozlov, and Nikita Malinin. Post-training deep neural network pruning via layer-wise calibration. *Proceedings of the IEEE/CVF International Conference on Computer Vision Workshops*, pages 798–806, 2021.
 - [6] Jaeho Lee, Sejun Park, Sangwoo Mo, Sungsoo Ahn, and Jinwoo Shin. LAMP: Extracting the hidden riches of linear anisotropic magnitude pruning. In *Advances in Neural Information Processing Systems*, volume 34, pages 10978–10990, 2021.
 - [7] Markus Nagel, Mart van Baalen, Tijmen Blankevoort, and Max Welling. Data-free quantization through weight equalization and bias correction. In *Proceedings of the IEEE/CVF International Conference on Computer Vision*, pages 1325–1334, 2019.
 - [8] Markus Nagel, Rana Ali Amjad, Mart van Baalen, Christos Louizos, and Tijmen Blankevoort. Up or down? adaptive rounding for post-training quantization. In *Proceedings of the 37th International Conference on Machine Learning*, pages 7197–7206. PMLR, 2020.
 - [9] Hao Yu et al. Statistical energy compensation for post-training LLM pruning. *arXiv preprint*, 2026.
 - [10] Qishi Zhan, Ziheng Chen, and Minxuan Hu. Adaptive signal resuscitation: Channel-wise post-pruning repair for sparse vision networks, 2026. URL <https://arxiv.org/abs/2605.21426>.